THE JOURNAL OF BIOLOGICAL CHEMISTRY VOL. 292, NO. 13, pp. 5519–5531, March 31, 2017
© 2017 by The American Society for Biochemistry and Molecular Biology, Inc. Published in the U.S.A.

Molecular Insights into Hydrogen Peroxide-sensing Mechanism of the Metalloregulator MntR in Controlling Bacterial Resistance to Oxidative Stresses*[S]

Received for publication, October 20, 2016, and in revised form, January 28, 2017 Published, JBC Papers in Press, February 21, 2017, DOI 10.1074/jbc.M116.764126

Zhaoyuan Chen[‡§], **Xinhui Wang**[‡§], **Fan Yang**[¶], **Qingqing Hu**[‡§], **Huichun Tong**[‡§1], **and Xiuzhu Dong**[‡§2]

From the [‡]*State Key Laboratory of Microbial Resources, Institute of Microbiology, Chinese Academy of Sciences, No.1 Beichen West Road, Chaoyang District, Beijing 100101, China,* [§]*School of Life Sciences, University of Chinese Academy of Sciences, No.19A Yuquan Road, Shijingshan District, Beijing 100049, China, and* [¶]*MOE Key Laboratory of Bioinformatics, School of Life Sciences, Tsinghua University, Beijing 100084, China*

Edited by Charles E. Samuel

Manganese contributes to anti-oxidative stress particularly in catalase-devoid bacteria, and DtxR family metalloregulators, through sensing cellular Mn^{2+} content, regulate its homeostasis. Here, we show that metalloregulator MntR (So-MntR) functions dually as Mn^{2+} and H_2O_2 sensors in mediating H_2O_2 resistance by an oral streptococcus. H_2O_2 disrupted So-MntR binding to Mn^{2+} transporter *mntABC* promoter and induced disulfide-linked dimerization of the protein. Mass spectrometry identified Cys-11/Cys-156 and Cys-11/Cys-11 disulfide-linked peptides in H_2O_2-treated So-MntR. Site mutagenesis of Cys-11 and Cys-156 and particularly Cys-11 abolished H_2O_2-induced disulfide-linked dimers and weakened H_2O_2 damage on So-MntR binding, indicating that H_2O_2 inactivates So-MntR via disulfide-linked dimerization. So-MntR C123S mutant was extremely sensitive to H_2O_2 oxidization in dimerization/oligomerization, probably because the mutagenesis caused a conformational change that facilitates Cys-11/Cys-156 disulfide linkage. Intermolecular Cys-11/Cys-11 disulfide was detected in C123S/C156S double mutant. Redox Western blot detected So-MntR oligomers in air-exposed cells but remarkably decreased upon H_2O_2 pulsing, suggesting a proteolysis of the disulfide-linked So-MntR oligomers. Remarkably, elevated C11S and C156S but much lower C123S proteins were detected in H_2O_2-pulsed cells, confirming Cys-11 and Cys-156 contributed to H_2O_2-induced oligomerization and degradation. Accordingly, in the C11S and C156S mutants, expression of *mntABC* and cellular Mn^{2+} decreased, but H_2O_2 susceptibility increased. In the C123S mutant, increased *mntABC* expression, cellular Mn^{2+} content, and manganese-mediated H_2O_2 survival were determined. Given the wide distribution of Cys-11 in streptococcal DtxR-like metalloregulators, the disclosed redox regulatory function and mechanism of So-MntR can be employed by the DtxR family proteins in bacterial resistance to oxidative stress.

Manganese is essential for organisms in the resistance of oxidative stresses (1–3) and required by many pathogenic bacteria for virulence and persistence in infected hosts (4–7). Manganese ion not only serves as a cofactor of superoxide dismutase but also forms non-proteinaceous manganese antioxidants by complexing with orthophosphate, lactate, or other small molecules (8–10). It is even found that cellular Mn^{2+} assists bacteria in γ-radiation resistance, which is virtually a tolerance to reactive oxygen species generated by ionizing radiation (11). Manganese antioxidants play particularly important roles in catalase void *Lactobacillus* and streptococci (4, 8, 12, 13). Acquisition of manganese is also crucial for virulence of *Streptococcus* pathogens like *Streptococcus pneumoniae* and *Streptococcus pyogenes*, most likely because manganese-antioxidants equip the bacterial pathogens for survival against the oxidants generated by the infected hosts (4, 6).

Manganese transportation is tightly controlled by metalloregulators because of the high cellular toxicity of the manganese ions when at excess concentration. Bacteria employ metal ion-dependent transcriptional regulators to control metal ion homeostasis, mainly through control of metal ion transport in or out of cells (14, 15). Through activating or suppressing the expression of divalent metal ion transporter genes, metalloregulators are responsible for the regulatory mechanisms of metal ion uptake and efflux that ensure sufficient cellular metal ions for bacteria metabolism and oxidative resistance while avoiding the toxic effect to cells (16–20). Recently, metalloregulators are found to regulate virulence gene expression in pathogenic bacteria (21, 22), making them the promising therapeutic targets in controlling pathogen infection. The streptococcal DtxR/MntR family metalloregulator homologues, including SloR from *Streptococcus mutans* (23), ScaR from *Streptococcus gordonii* (24), and PsaR from *S. pneumoniae* (25) are affiliated with the manganese/iron type of metalloregulators. They all repress Mn^{2+} transport by sensing cellular Mn^{2+} sufficiency to prevent excess metal toxicity, *e.g.* PsaR acts as the Mn^{2+}-dependent repressor of the Mn^{2+} importer *psaABC* and the virulent genes *prtA* and *pcpA* (26), and ScaR suppresses the virulence-related Mn^{2+} permease *scaCBA* operon expression by sensing cellular Mn^{2+} concentration (24). The structural studies of ScaR, SloR, and PsaR in the presence of Cd^{2+} or Zn^{2+}

* This work was supported by National Natural Science Foundation of China Grant 31370098. The authors declare that they have no conflicts of interest with the contents of this article.
[S] This article contains supplemental Tables S1–S4 and Figs. S1–S3.
[1] To whom correspondence may be addressed. Tel.: 86-10-6480-7567; Fax: 86-10-6480-7429; E-mail: tonghuichun@im.ac.cn.
[2] To whom correspondence may be addressed. Tel.: 86-10-6480-7413; Fax: 86-10-6480-7429; E-mail: dongxz@im.ac.cn.

This is an Open Access article under the CC BY license.

reveal that Cys-123 is one of the key residues for metal ion binding (27–29).

Given the essentiality of Mn^{2+} for the protection of bacteria from oxidative harm, it is crucial to understand how these DtxR-like metalloregulators regulate Mn^{2+} import by sensing cellular redox status (H_2O_2 level). *Streptococcus oligofermentans* is a beneficial oral commensal and generates a high concentration of H_2O_2 to inhibit the growth of dental caries pathogen *S. mutans* and also tolerates a high amount of H_2O_2 (30–32). Although previously we found that in response to H_2O_2, the peroxide-responsive repressor PerR de-represses the expression of *mntABC* gene that encodes a Mn^{2+} uptake transporter in *S. oligofermentans* (13), a direct connection between PerR and *mntABC* has not been found.

In the present study we identified a ScaR/PsaR homolog, tentatively named $mntR_{So}$, in the *S. oligofermentans* genome. By sensing intracellular Mn^{2+} concentration, So-MntR directly repressed the expression of the Mn^{2+} transporter operon *mntABC*. In the following redox proteome study, to screen the redox-sensitive cysteines in H_2O_2-pulsed *S. oligofermentans*, it was found that all three cysteines of the So-MntR protein were oxidized to form disulfide bond.[3] This suggests that So-MntR can be a metalloregulator in control Mn^{2+} uptake by sensing oxidative stress. In the present study we, through redox biochemistry, genetic, and physiological studies, demonstrated that in response to H_2O_2, $mntR_{So}$ de-represses the expression of *mntABC* and facilitates Mn^{2+} import; we also found that H_2O_2 inactivates So-MntR. The cellular So-MntR oligomers appear to be readily degraded and so cause de-repression of *mntABC* and an increase of Mn^{2+} import. Thus, this work provides a new mechanism of a metalloregulator contributing to oxidative stress resistance in response to H_2O_2.

Results

S. oligofermentans MntR Suppressed mntABC Expression and Mn^{2+} Import by Sensing Both the Cellular Mn^{2+} and Redox Status—To search the ScaR/PsaR ortholog in *S. oligofermentans*, *scaR* from *S. gordonii* (SGO_1816) was used as a probe to query the completed *S. oligofermentans* genome. A gene (I872_01020) annotated as "DtxR family manganese-dependent transcriptional regulator" was hit at a 73.8% identity with *scaR*. Similar to ScaR, this 25-kDa protein possessed three domains: an N-terminal DNA binding domain, a central metal binding and dimerization domain, and a C-terminal FoeA domain. Moreover, it contained the conserved metal ion binding amino acids that present in the ScaR-like DtxR homologues from streptococci (27), namely Asp-7, Glu-99, Glu-102, and His-103 (the primary site) and Glu-80, Cys-123, His-125, and Asp-160 (the secondary site) (Fig. 1*A*). Thus this gene was tentatively assigned as $mntR_{So}$ and So-MntR of the encoded protein. A protein superimposition of the So-MntR homology model and the dimeric crystal structure of ScaR (3hrs.1.pdb, X-ray diffraction at 2.70 Å) also showed good matching (Fig. 1*B*).

To confirm the regulatory role of So-MntR in transport of Mn^{2+} and other metal ions, a $mntR_{So}$ deletion strain was constructed by means of double-crossover recombination. Inductively coupled plasma mass spectrometry (ICP-MS)[4] was used to determine the cellular content of metal ions in the wild strain and $mntR_{So}$ mutant that grows in brain heart infusion (BHI) broth supplemented with a variety of concentrations of $MnCl_2$. As shown in supplemental Table S1, deletion of $mntR_{So}$ caused an ~1.5-fold increased cellular Mn^{2+} content in the presence of ≤3 μM $MnCl_2$ and a 3-fold increase with a 100 μM and 5 mM $MnCl_2$ supply. Correspondingly, $mntR_{So}$ deletion decreased *S. oligofermentans* Mn^{2+} tolerance, and growth was significantly suppressed by 5 mM Mn^{2+}, whereas the wild type tolerated up to 5 mM Mn^{2+} (supplemental Fig. S1). Noticeably, the cellular iron level was also increased in the $mntR_{So}$ mutant. Cellular iron content decreased as the manganese supply increased (supplemental Table S1), implying that the Mn^{2+} transporter prefers manganese uptake.

Previously, we determined that MntABC is the major Mn^{2+} transporter of *S. oligofermentans* (13). To link So-MntR-controlled Mn^{2+} uptake with the immediate regulation of Mn^{2+} transporters, *mntABC* expression was measured in luciferase reporter strains WT-P*mntABC-luc* (13) and Δ$mntR_{So}$-P*mntABC-luc*. As expected, in comparison with the wild strain, *mntABC* expression increased 3.2- and 4.6-fold in Δ$mntR_{So}$-P*mntABC-luc* strain that cultured statically or anaerobically in BHI broth (supplemental Table S2), respectively. When growing the two reporter strains, a given concentration of $MnCl_2$ or $FeSO_4$ in a metal ion-deprived BHI (B-BHI) broth, luciferase activity assay did not detect a significant repression of $mntR_{So}$ on *mntABC* unless the addition was ≥0.5 μM Mn^{2+}. However, even up to 200 μM, ferrous ion did not activate $mntR_{So}$ repression of *mntABC* (supplemental Table S2). This indicated that manganese is the cognate ligand of So-MntR. Surprisingly, only half the level of *mntABC* expression was determined in an anaerobic culture (luciferase activity, $1.05 \pm 0.17 \times 10^6$ relative light units (RLU)/A_{600}) compared with the statically cultured cells ($2.01 \pm 0.35 \times 10^6$ RLU/A_{600}). This implies that So-MntR may also sense redox potential in controlling *mntABC* expression. Taken together, So-MntR suppression of *mntABC* requires Mn^{2+} as the ligand and responds to oxidation status.

H_2O_2 Decreased Mn^{2+}-dependent Binding of So-MntR to mntABC Promoter—To characterize So-MntR protein, it was overexpressed in *Escherichia coli* and purified. Size exclusion chromatography showed that So-MntR molecular mass was ~50 kDa, indicating that it presents a dimer in the solution (supplemental Fig. S2). Next, electrophoretic mobility shift assay (EMSA) was performed to determine the direct association of So-MntR and *mntABC*. Fig. 2*A* showed that in the presence of 100 μM Mn^{2+}, as low as 5 nM So-MntR protein bound to the promoter of *mntABC*, and a dose-dependent protein-DNA complex formation was observed. The shifted DNA bands were abolished by the addition of increased unlabeled *mntABC* promoter into the binding mixture. However, no DNA shift was found in the absence of Mn^{2+}, indicating that So-MntR specifically binds to *mntABC* promoter by using Mn^{2+} as the ligand.

[3] Z. Chen, X. Wang, F. Yang, Q. Hu, H. Tong, and X. Dong, unpublished data.

[4] The abbreviations used are: ICP-MS, inductively coupled plasma-MS; BHI, brain heart infusion; NEM, *N*-ethylmaleimide; RIPA, radioimmune precipitation assay; qPCR, quantitative-PCR.

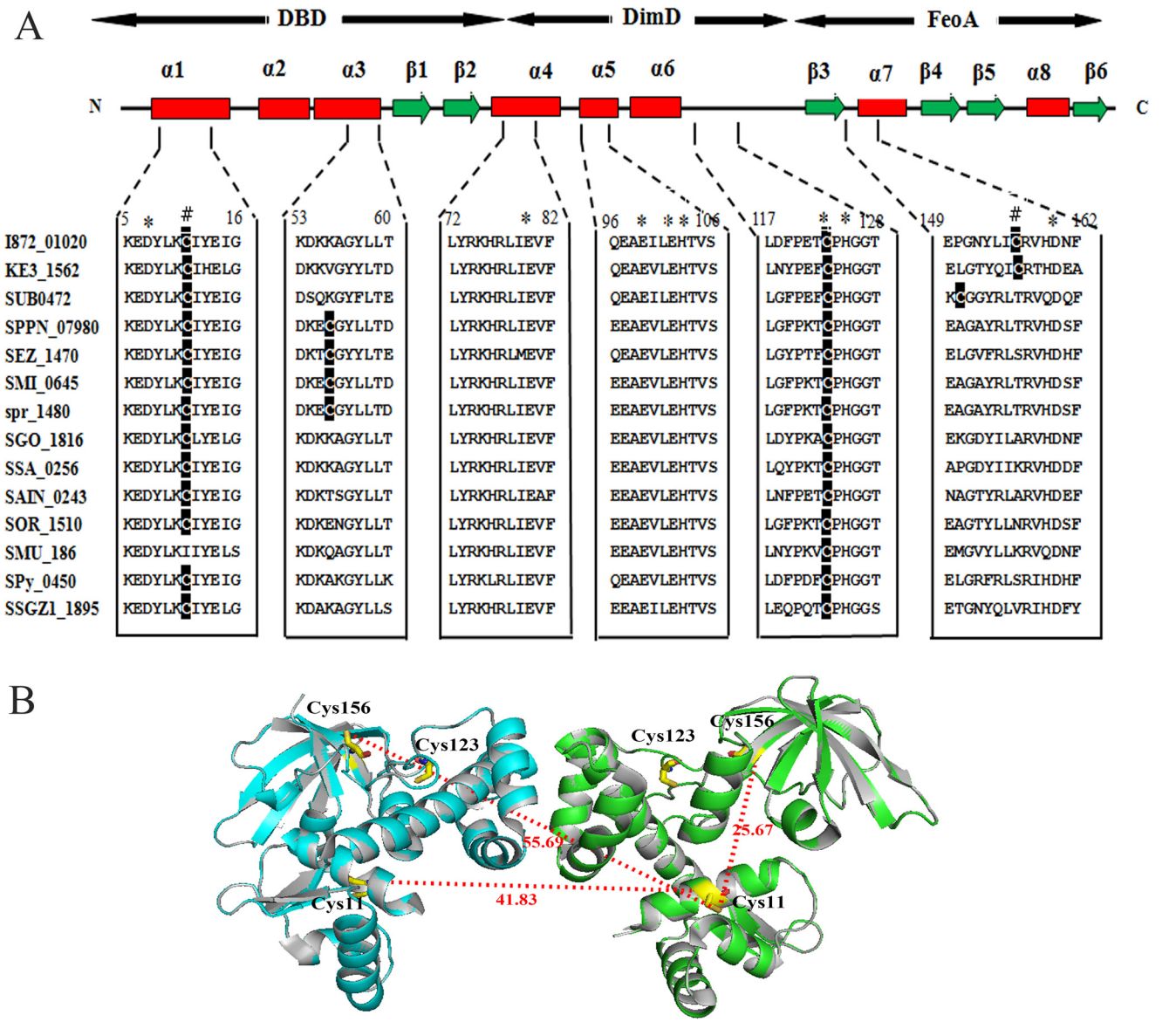

FIGURE 1. **Multiple sequence alignment of DtxR family homologues from streptococci (*A*) and superimposition of So-MntR over ScaR (*B*).** *A*, protein sequences are retrieved from the protein database of NCBI and aligned using ClustalW2. *DBD*, DNA binding domain; *DimD*, metal binding and dimerization domain; *FeoA*, FeoA domain. The secondary structure of ScaR (SGO_1816) (27) was used to indicate the amino acids position. *Numbers on the top of the sequences* represent the corresponding amino acids position in the So-MntR. *, conserved amino acid residues essential for metal ion binding in ScaR-like DtxR homologues (Asp-7, Glu-99, Glu-102, and His-103 in the primary site; Glu-80, C123, His-125, and Asp-160 in the secondary site). #, H_2O_2-sensitive cysteine residues in *S. oligofermentans* MntR. I872_01020: *S. oligofermentans*; KE3_1562: *S. lutetiensis*; SUB0472: *S. uberis*; SPPN_07980: *S. pseudopneumoniae*; SEZ_1470: *S. equi* subsp. *Zooepidemicus*; SMI_0645: *Streptococcus mitis*; Spr_1480: *S. pneumoniae*; SGO_1816: *S. gordonii*; SSA_0256: *Streptococcus sanguinis*; SAIN_0243: *Streptococcus anginosus*; SOR_1510: *Streptococcus oralis*; SMU_186: *S. mutans*; SPy_0450: *S. pyogenes*; SSGZ1_1895: *Streptococcus suis*. *B*, the homo-dimer homology model of *S. oligofermentans* MntR was generated via the SWISS-MODEL web server by automatically matching 3hrs.1.pdb, a dimeric crystal structure of ScaR from *S. gordonii*, as template. The dimeric So-MntR (two monomers shown in blue and green, respectively) was overlaid with ScaR (*gray*). The three cysteine residues were shown as sticks, and the distance (Å) between each pair was predicted with PyMOL.

Given that a higher *mntABC* expression occurred in static than in anaerobic culture (supplemental Table S2) and that *S. oligofermentans* generates endogenous H_2O_2 in the presence of O_2 (30, 31, 33), we then decided to test H_2O_2 impact on So-MntR binding to the *mntABC* promoter. Fifteen nanomolar So-MntR protein was incubated with various concentrations of H_2O_2 for 90 min and terminated the oxidation by catalase. The oxidized So-MntR was then used for EMSA in the presence of Mn^{2+}. As shown in Fig. 2*B*, 0.1 mM H_2O_2 treatment severely decreased So-MntR binding to the *mntABC* promoter, whereas 1 mM H_2O_2 completely abolished the binding. When various concentrations of H_2O_2 were added after the binding of So-MntR protein (15 nM) to the *mntABC* promoter, it was found that 0.1 and 1 mM H_2O_2, respectively, caused partial and complete dissociation of So-MntR from the target DNA (Fig. 2*C*). Interestingly, the H_2O_2-disrupted binding complex was mostly recovered by 10 mM 1,4-dithiothreitol (DTT) treatment, indicating an involvement of reversible disulfide formation upon H_2O_2 oxidation (Fig. 2*C*). To avoid possible Fenton chemistry damage, the So-MntR-His_6 protein was purified and dialyzed in the presence of 1 mM EDTA, and treated with 10 g/liter Chelex 100 to remove metal ions at the last dialysis. Metal ion content

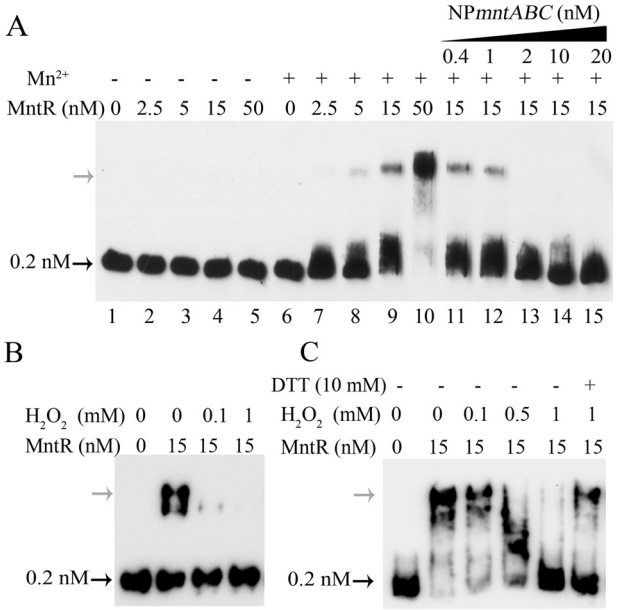

FIGURE 2. **Impact of H_2O_2 on So-MntR binding to the *mntABC* promoter.** *A*, Mn^{2+} facilitated a specific binding of So-MntR to *mntABC* promoter. DNA fragment of the *mntABC* promoter was PCR-amplified with 5′-end biotin-labeled primers. Various concentrations of So-MntR protein were added to the EMSA binding mixture in the absence (*lane 1–5*) or presence (*lane 6–15*) of 0.1 mM $MnCl_2$. The addition of increased concentrations of non-labeled DNA probe (NP*mntABC*) (*lanes 11–15*) decreased the protein-DNA complex and completely diminished it at a 10-fold NP*mntABC* supplementation. *B*, H_2O_2 weakened So-MntR binding to the *mntABC* promoter. 15 nM concentrations of So-MntR were incubated with 0.1 and 1 mM H_2O_2 for 90 min. After catalase stopped the reaction, oxidized So-MntR was tested for binding to the *mntABC* promoter by EMSA as described under "Experimental Procedures." *C*, H_2O_2 dissociated So-MntR from the *mntABC* promoter. So-MntR protein was allowed to bind to the *mntABC* promoter in the presence of 0.1 mM $MnCl_2$, and then 0.1, 0.5, and 1 mM H_2O_2 was added to the binding mixture. After 90 min of H_2O_2 treatment, catalase was added, and one reaction was treated with DTT. EMSA was performed to examine the protein-DNA association. *Gray* and *black arrows* indicate the protein-DNA complexes and free DNA fragment, respectively.

in the So-MntR-His_6 was then measured using ICP-MS, which detected only trace amounts of transition metal ions in 15 nM protein with iron (0.09 nM), cobalt (0.0003 nM), copper (0.018 nM), and manganese (0.0015 nM).

H_2O_2 Facilitated Disulfide-linked So-MntR Dimers—So-MntR contains three cysteine residues (Fig. 1*A*), and the thiol groups can be oxidized by H_2O_2 to form a disulfide bond. Dimers were indeed observed for the purified So-MntR on denaturing non-reducing SDS-PAGE gel. Therefore, H_2O_2 oxidation on So-MntR disulfide-linked dimer formation was further analyzed. Fig. 3*A* showed that after 90 min of treatment with 0.1 mM H_2O_2, an ~4-fold increase in dimer formation (*lane 1 versus lane 4*) as well as slightly increased disulfide-linked monomers were noted. The dimer bands were all abolished by DTT reduction (Fig. 3*B*), indicating that H_2O_2-induced dimers are formed via disulfide bond linkage. Mn^{2+} appeared to counteract H_2O_2-induced So-MntR dimerization by decreasing the ratio of dimer to monomer from 0.74 to 0.44 (*lane 4 versus lane 5*, Fig. 3*A*). To avoid incorrect disulfide linkages induced during protein denaturation, So-MntR was pretreated with *N*-ethylmaleimide (NEM), a thiol alkylating agent, to block the free thiol groups before being subjected to non-reducing SDS-PAGE gel. Notably, disulfide-linked dimers/oligomers frequently occurred in So-MntR without H_2O_2 treatment (*lane 1*, Fig. 3*A*), suggesting that this protein is extremely liable to air oxidation.

To determine the disulfide bond linkages in H_2O_2-treated So-MntR, the dimer and disulfide-linked monomer bands (Fig. 3*A*, *lanes 1* and *4*) were excised and subjected to LC-MS/MS analysis. Iodoacetamide was used to block the free thiol groups before trypsin digestion of the gel. Cys-11/Cys-11, Cys-11/Cys-156, and Cys-156/Cys-156 fragments were all identified in the dimers, whereas Cys-11/Cys-156 and Cys-11/Cys-11 were overrepresented in H_2O_2-treated protein according to the increased disulfide-linked peptide spectral matches numbers compared with the untreated protein (supplemental Table S3). Fig. 3*C* shows the representative MS/MS spectrometric maps in which Cys-11/Cys-11 and Cys-11/Cys-156 disulfide linkages were each identified as a 3-charged peptide fragment of CIYEIGTRQEK/CIYEIGTR (observed *m*/*z* of 764.378) and CIYEIGTR/YHQSLASAQEPGNYLICR (observed *m*/*z* of 1001.151), respectively. In disulfide-linked monomer only Cys-11/Cys-156 peptide was identified (supplemental Table S3). Noticeably, the intramolecular Cys-11/Cys-156 linkage appeared to change the protein conformation by migrating faster than the common monomer (band *im*, Fig. 3*A*). Cys-123 seemed not to involve either the inter- or the intramolecular disulfide bond; likely it is involved in Mn^{2+} binding as in other DtxR-like metalloregulators (27).

Cys-11 and Cys-156 Contribute to H_2O_2-induced Disulfide-linked Dimerization and So-MntR Inactivation, Whereas Cys-123 Linked to DNA Binding—To verify the contribution of each cysteine to the disulfide linked dimers, we mutated each of the three residues to serine and examined dimerization in H_2O_2-treated mutant proteins. A non-reducing SDS-PAGE (Fig. 4*A*) assay showed that mutation of Cys-11 completely eliminated the dimerization, whereas the Cys-156 mutation reduced the dimers but increased oligomers. This indicates that both Cys-11 and Cys-156 are involved in disulfide-linked dimerization. In contrast, in response to H_2O_2 treatment, the So-MntR C123S mutant substantially increased both intra- and intermolecular disulfide bond linkages. To further determine the relative level of same cysteine disulfide-linked dimers, C11S and C156S mutagenesis was each introduced into So-MntR C123S mutant to generate double cysteine mutagenesis. As shown in Fig. 4*A*, either the C11S/C123S or C156S/C123S double mutants (dimer:monomer = 0.10) produced ~8.7-fold less disulfide-linked oligomers than that the C123S mutant (dimer: monomer = 0.87) upon H_2O_2 treatment. This indicates that same cysteine disulfide linkage between Cys-11/Cys-11 and Cys-156/Cys-156 would contribute 20% of the S-S dimers, and Cys-11/Cys-156 contributes the remaining 80%. Noticeably, there were more disulfide-linked di- and oligomers in C123S mutant, implying that C123S mutagenesis might change the So-MntR conformation, thereby facilitating the interaction of Cys-11 and Cys-156. Circular dichroism (CD) spectra analysis did show a dramatic secondary structure change for the C123S mutant that reduced the α helix (from 39% in the wild protein to 24%) but increased the β strand content (from 17% in the wild protein to 28%). There was only a slight conformation change for the C11S and C156S mutants (supplemental Fig. S3).

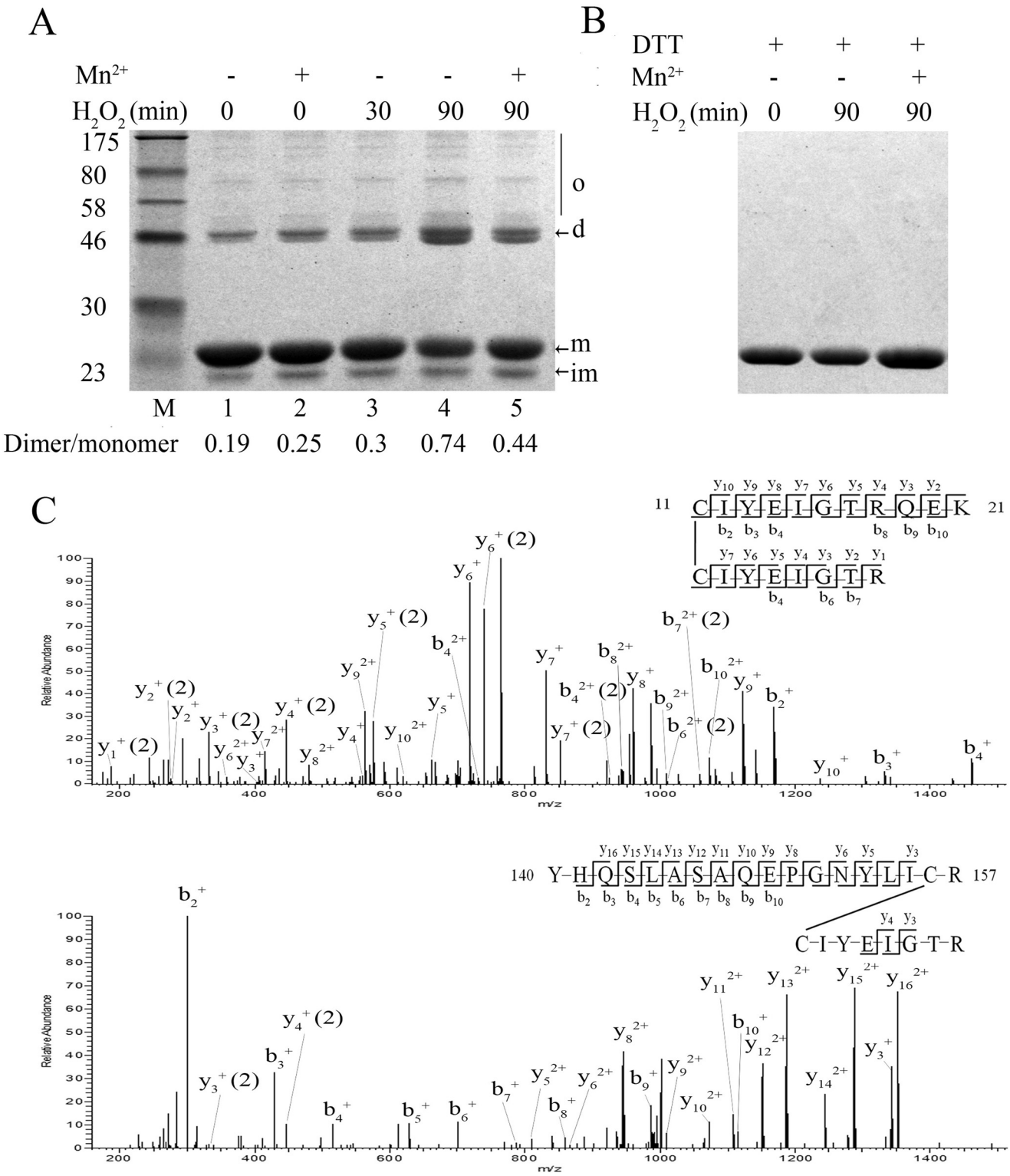

FIGURE 3. **Determination of the disulfide-linked dimers and peptides in H_2O_2-treated So-MntR.** *A*, non-reducing SDS-PAGE detected H_2O_2-induced disulfide-linked dimers of So-MntR. Five micrograms of So-MntR protein was treated with 0.1 mM H_2O_2 for the indicated time periods *above each lane* in the presence or absence of 0.1 mM $MnCl_2$. As the H_2O_2 treatment period prolonged, dimer (*d*) content increased and monomer (*m*) decreased (*lanes 4* and *5*). The ratio of dimer to monomer was shown *beneath each lane*, which was calculated based on the densities of the respective band. *B*, addition of 10 mM DTT to H_2O_2-treated MntR; only the monomer was retained. *C*, LC-MS/MS identification of disulfide-linked peptides. Representative MS/MS fragmentation of the ion at *m/z* 764.3784 corresponding to the disulfide-linked peptide fragment Cys-11/Cys-11 (*upper panel*) and *m/z* 1001.151 corresponding to the peptide fragment containing Cys-11/Cys-156 (*lower panel*). The insets in each MS/MS spectrogram showed the graphic fragment map of the relevant peptide sequence matching with the observed fragmentation ion.

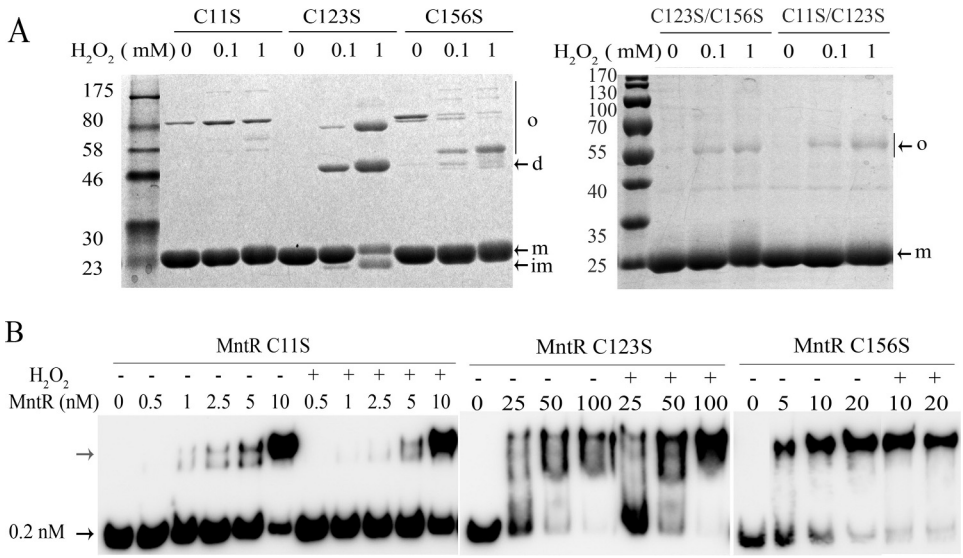

FIGURE 4. **Contribution of each cysteine residue to So-MntR H_2O_2 sensitivity.** *A*, non-reducing SDS-PAGE determined H_2O_2-induced disulfide-linked dimer of the wild type and cysteine-mutated So-MntR. By using the same procedure as Fig. 3*A*, 5 μg of the wild type So-MntR and each of three cysteine residue single or double mutants were treated with 0.1 mM and 1 mM H_2O_2 for 90 min, respectively. *d*, *o*, *m*, and *im* are as in Fig. 3*A*. *B*, EMSA assayed each cysteine-mutated So-MntR binding to the *mntABC* promoter in response to 0.1 mM H_2O_2.

Next, impact of cysteine mutation on So-MntR binding to DNA was detected by EMSA. Cys-11 mutation remarkably increased So-MntR affinity to DNA by showing binding at as low as 1 nM protein (Fig. 4*B*), most likely because of its position in the DNA binding domain. By comparing the DNA binding ability change by H_2O_2 treatment, it was found that either C11S or C156S mutation reduced H_2O_2 damage on So-MntR affinity to DNA, indicating that disulfide-linked dimer formation causes So-MntR inactivation (Fig. 4*B*). In addition, C123S mutation reduced about half of the DNA affinity regardless of H_2O_2 oxidation, indicating that this residue contributes DNA binding.

H_2O_2-induced Disulfide-linked Oligomerization Caused Cellular So-MntR Decrease—To test the intracellular So-MntR status, we constructed the *S. oligofermentans* $mntR_{So}$-His_6 strain by inserting the C-terminal-His_6-tagged $mntR_{So}$ into shuttle vector pDL278 (34) and transformed it into the $mntR_{So}$ deletion strain. The anaerobically cultured $\Delta mntR_{So}$-*mntR* cells at the middle exponential phase were harvested and divided into four aliquots. Two aliquots were exposed to air for 30 or 60 min, 1 was air-exposed but with 200 μg/ml catalase addition, and another aliquot was retained anaerobically. Cell samples were then sonicated in RIPA buffer containing NEM, and the supernatant was subjected to redox-Western hybridization using anti-His-tag antibody. As shown in Fig. 5*A*, compared with the anaerobically stand sample, 30 min of air exposure caused more So-MntR oligomer, which became much less in the catalase-treated sample. This indicates that H_2O_2 oxidation contributes to the oligomer formation. Next, anaerobically cultured $mntR_{So}$-His_6 strain was treated with various concentrations of H_2O_2, and then the *in vivo* So-MntR level was determined as described above. It turned out that either 30 min of pulsing of 40 μM H_2O_2 or 5 min of pulsing of 120 μM H_2O_2 significantly increased both monomer and oligomer formation, whereas extending the 120 μM H_2O_2 pulsing to 10 or 30 min

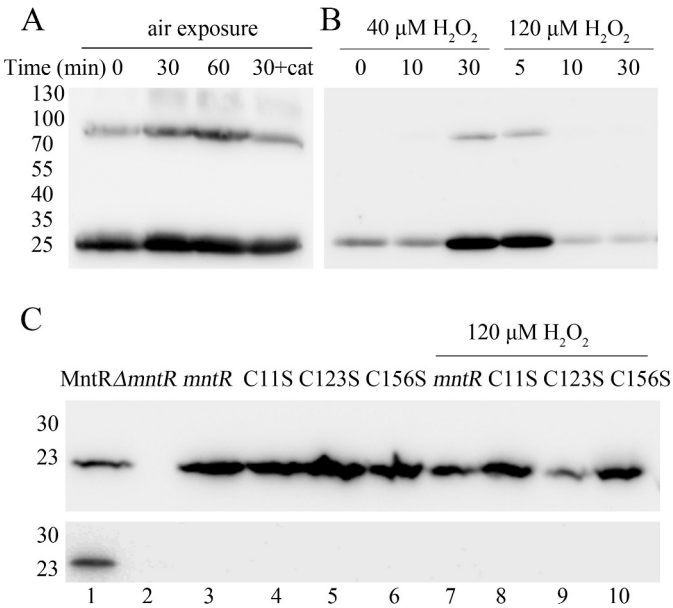

FIGURE 5. **Redox Western hybridization detected the wild and cysteine-mutated So-MntRs in H_2O_2-pulsed *S. oligofermentans* cells.** Strains were cultured anaerobically until the middle log phase, and aliquots of cultures were collected and treated as indicated above each figure. *A*, culture aliquots of the $\Delta mntR_{So}$-*mntR* strain were exposed to air for 30 or 60 min. +*cat*, catalase (200 μg/ml) was added to the culture. Cells were collected and sonicated in RIPA buffer containing the thiol alkylating agent NEM. After centrifugation, 50 μg of cellular protein were resolved by non-reducing SDS-PAGE, and a 4000-fold dilution of the anti-His-tag antiserum was used to probe the *in vivo* So-MntR protein. *B*, culture aliquots of the $\Delta mntR_{So}$-*mntR* strain were treated, respectively, with 40 or 120 μM H_2O_2 for the time indicated on the *top of each lane*. The cellular So-MntR was detected using the procedure as described in *A*. *C*, culture aliquots of the wild type and cysteine-mutated $mntR_{So}$-complemented strains were treated with 120 μM H_2O_2 for 30 min. The corresponding aliquots without H_2O_2 treatment were included as controls. Using the same approach as *A*, So-MntR proteins in cell extract supernatant (*upper panel*) and the pellet (*lower panel*) were examined by redox Western blot. *Lane 1*, purified recombinant So-MntR protein; *lane 2*, $\Delta mntR_{So}$-pDL278 strain; *lanes 3* and *7*, $\Delta mntR_{So}$-*mntR* strain; *lanes 4* and *8*, $\Delta mntR_{So}$-*mntR*C11S strain; *lanes 5* and *9*, $\Delta mntR_{So}$-*mntR*C123S strain; *lanes 6* and *10*, $\Delta mntR_{So}$-*mntR*C156S strain.

caused the oligomer to be diminished and the monomer to be decreased significantly as well (Fig. 5*B*). The redox Western hybridization data strongly suggest that under H_2O_2 stress cellular MntR forms inactive oligomers and are then subjected to a proteolysis. The monomer increase can be due to H_2O_2 induction of $mntR_{So}$ expression, found in an unpublished Microarray data.[3]

H_2O_2 induced cellular So-MntR dimerization/oligomerization, and vanishing was further tested on the cysteine-mutated $mntR_{So}$ mutants, which are insensitive to H_2O_2 oxidation in formation of dimers and oligomers. The $mntR_{So}$ deletion mutant was complemented with each of the three cysteine-mutated (C11S, C123S, and C156S) $mntR_{So}$-His$_6$s, designated as Δ$mntR_{So}$-*mntR*C11S, Δ$mntR_{So}$-*mntR*C123S, and Δ$mntR_{So}$-*mntR*C156S, respectively. These strains were grown anaerobically until mid-log phase and then subjected to 30 min of pulsing with 120 μM H_2O_2. Redox Western blot was performed to examine the So-MntR proteins in both the supernatant and precipitate of the cell extract. It was observed that upon H_2O_2 pulsing, So-MntR protein reduced by 33 and 65% in the Δ$mntR_{So}$-*mntR* and Δ$mntR_{So}$-*mntR*C123S strains, respectively. However, only a 14 and 25% decrease of So-MntR protein was noted in the Δ$mntR_{So}$-*mntR*C11S and Δ$mntR_{So}$-*mntR*C156S strains, respectively (Fig. 5*C*, *upper panel*). No So-MntR protein was detected in the cell extract precipitation of any tested strains (Fig. 5*C*, *lower panel*). This suggests that diminished So-MntR protein in the cell can be attributed to a proteolytic action. The H_2O_2 sensitivity of each So-MntR protein is in line with its tendency in dimerization/oligomerization (Fig. 4*A*).

So-MntR Cys-11 and Cys-156 Mutagenesis Decreased the mntA Gene Expression and Cellular Mn^{2+} Content in the Presence of H_2O_2—To further inspect the role of H_2O_2-sensitive cysteine in mediating So-MntR oxidative inactivation *in vivo*, expression of *mntA* (I872_09645, metal ABC transporter substrate binding lipoprotein) in Δ$mntR_{So}$-*mntR* and Δ$mntR_{So}$-*mntR*C11S, -C123S, and -C156S strains was quantified by quantitative-PCR (qPCR). Strains were cultured anaerobically in BHI broth until the $A_{600} \sim 0.4-0.5$ and then treated with 40 μM H_2O_2 for 30 min. Fig. 6 showed that upon H_2O_2 treatment ~2.8- and ~2.5-fold elevated *mntA* transcript was detected in Δ$mntR_{So}$-*mntR* and Δ$mntR_{So}$-C123S strains, respectively, whereas no significantly increase was detected in the Δ$mntR_{So}$-*mntR*C11S and C156S strains, indicating that the cysteine residues contribute to So-MntR repression of *mntABC* expression when encountering H_2O_2.

As MntABC functions in Mn^{2+} transport (13), ICP-MS was then used to determine the cellular Mn^{2+} content in Δ$mntR_{So}$-pDL278, Δ$mntR_{So}$-*mntR*, and Δ$mntR_{So}$-*mntR*C11S, -C123S, and -C156S strains. Strains were all grown statically in either BHI broth or BHI supplemented with 0.1 mM $MnCl_2$. Under either culture conditions, a significantly reduced intracellular Mn^{2+} was detected in the Δ$mntR_{So}$-*mntR*C11S and C156S strains (Table 1). This is consistent with the reduced *mntABC* expression in the Δ$mntR_{So}$-*mntR*C11S and -C156S mutants that retained more So-MntR protein in the cell (Figs. 6 and 5*C*).

So-MntR Mediated Manganese-dependent Anti-oxidative Stress Based on the H_2O_2-reactive Cys-11 and Cys-156—To examine the effect of $mntR_{So}$ deletion and So-MntR cysteine

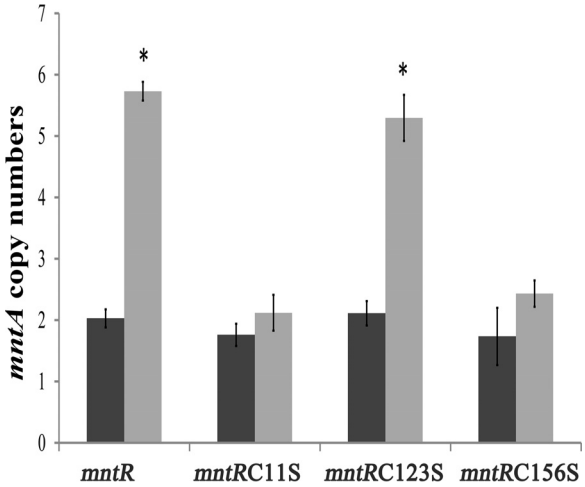

FIGURE 6. **H_2O_2-induced *mntA* expression in the wild and cysteine-mutated $mntR_{So}$ ectopically expressed strains.** Strains were cultured anaerobically in BHI broth until $A_{600} \sim 0.4-0.5$, and then 1 aliquot of cells was treated with 40 μM H_2O_2 for 30 min, leaving another aliquot untreated. Cells were collected, and total RNA was extracted. Using qPCR as described under "Experimental Procedures," the transcript abundance of *mntA* gene was quantified. *Black bars*, anaerobically cultured cells; *gray bars*, H_2O_2 treated cells. *, significant difference was determined between H_2O_2 treated and not treated cells ($p < 0.05$, Student's *t* test). The experimental data were from three batches of cells and repeated three times for each sample. The results represent the average ± S.D. of the copy number/0.001 16S rRNA gene copy from three independent experiments.

mutation on manganese-mediated H_2O_2 survival of *S. oligofermentans*, the above strains were grown in either BHI broth or BHI supplemented with 0.1 mM $MnCl_2$. When the growth reached $A_{600} \sim 0.4$, 1 aliquot of each culture was exposed to 10 mM H_2O_2 for 10 min while leaving another aliquot untreated. H_2O_2 survival rate was determined by the percentage of colony forming units (cfu) in H_2O_2-exposed aliquots against those in non-exposed aliquots. As shown in Table 1, in the presence of 0.1 mM $MnCl_2$, all strains significantly increased the H_2O_2 survival rates compared with their counterparts grown in BHI (containing approximate 500 nM Mn^{2+}). The $mntR_{So}$ deletion strain displayed ~2-fold elevated H_2O_2 survival rate compared with the wild strain. Consistent with the maximal H_2O_2-induced MntR degradation when Cys-123 was mutated, this mutant exhibited ~2-fold higher H_2O_2 survival than the wild strain (Table 1). Cys-11 was most sensitive to H_2O_2, and its mutation led to decreased cellular Mn^{2+} content and H_2O_2 survival. Taken together, the physiological evidence demonstrates that the metalloregulator So-MntR, via H_2O_2-induced disulfide-linked di-/oligomerization between the redox-sensitive cysteine, regulates H_2O_2 resistance of *S. oligofermentans* on the basis of Mn^{2+} transport control.

The H_2O_2-reactive Cysteine Residues Are Widely Distributed in DtxR Family Metalloregulators from Streptococci—To find the applicability of H_2O_2-responded disulfide linkage inactivation in DtxR family proteins, amino acid sequences of So-MntR and DtxR homologues from streptococci were aligned using ClustalW2 (Fig. 1*A*) to survey the distribution of H_2O_2-reactive cysteine residues. Cys-11, positioned at the DNA binding domain, is present in all the streptococcal DtxR homologues except for *S. mutans* SloR. Cys-123, a predicted metal ion binding residue situated in the dimerization domain, is widely

TABLE 1

Effect of each cysteine mutation of *mntR*$_{So}$ on the cellular manganese content and Mn^{2+}-mediated H_2O_2 survival of *S. oligofermentans*

Data are the means ± S.D. of three independent experiments. Suffixes of the Δ*mntR*$_{So}$ represent the complemented gene types of the *mntR*$_{So}$, and pDL278 indicates an empty vector only.

Measured items	Δ*mntR*$_{So}$-pDL278	Δ*mntR*$_{So}$-*mntR*	Δ*mntR*$_{So}$-*mntR*C11S	Δ*mntR*$_{So}$-*mntR*C123S	Δ*mntR*$_{So}$-*mntR*C156S
Manganese content[a]					
BHI + $MnCl_2$	7.33 ± 2.23[b]	3.65 ± 0.02	2.88 ± 0.10[b]	3.39 ± 0.09	2.97 ± 0.16[b]
BHI	2.59 ± 0.37[b]	1.66 ± 0.14	0.61 ± 0.15[b]	0.65 ± 0.37[b]	0.82 ± 0.23[b]
H_2O_2 survival (%)[c]					
BHI + $MnCl_2$	19.18 ± 1.84[b]	12.91 ± 3.04	6.47 ± 1.33[b]	23.11 ± 0.81[b]	11.24 ± 2.46
BHI	4.48 ± 0.54[b]	1.76 ± 0.38	0.79 ± 0.42[b]	0.99 ± 0.51	0.61 ± 0.17[b]

[a] Cellular manganese content (nmol/mg of protein) of tested strains grown statically in BHI broth or BHI supplemented with 0.1 mM $MnCl_2$.
[b] Data are significantly different from that in the Δ*mntR*$_{So}$-*mntR* strain ($p < 0.05$, Student's *t* test).
[c] H_2O_2 survival rate (%) of tested strains anaerobically grown in BHI broth with or without addition of 0.1 mM $MnCl_2$.

distributed in all the DtxR-like proteins from streptococci, whereas Cys-156 presents only in the MntR of *S. oligofermentans* and *Streptococcus lutetiensis* (35). Of note, a group of streptococcal DtxR homologues, including those derived from pathogen *S. pneumoniae*, *Streptococcus pseudopneumoniae* and *Streptococcus equi*, contain the 3rd cysteine at position 57 associated to the DNA binding domain. This implies that the DtxR family proteins from streptococci might all be H_2O_2-reactive.

Discussion

Metal homeostasis plays a central role in the anti-oxidative stress of Gram-positive bacteria particularly of the catalase void lactic acid bacteria (1, 2, 4, 12). Metalloregulators are the key controllers in maintaining bacterial metal homeostasis by sensing the cellular metal redundancy or deficiency (14, 15, 36). This work presents that a manganese homeostasis regulator MntR, by sensing the cellular oxidant, de-represses the Mn^{2+} transporter *mntABC* expression and enables an oral commensal *S. oligofermentans* to resist oxidative stress. Fig. 7 shows the working mechanism of the *S. oligofermentans* MntR. By sensing the cellular Mn^{2+} redundancy, So-MntR represses the expression of *mntABC*, the major Mn^{2+} importer. When encountering H_2O_2 stress either from the metabolic accumulation or from external source, So-MntR is oxidized at the redox-reactive thiol groups of Cys-11 and/or Cys-156 to form disulfide-linked dimers or oligomers, which can be subjected to a proteolysis. Depletion of the cellular MntR protein leads to *mntABC* de-repression and increased Mn^{2+} uptake and consequently facilitates the bacterium manganese-mediated resistance of oxidative stress.

Streptococci are well known for accumulating high cellular H_2O_2 due to a lack of catalase. Therefore, they have evolved unusual protective approaches from oxidative stress. Maintaining metal ion homeostasis is one of the important strategies (2, 13). Streptococci usually use Mn^{2+} instead of Fe^{2+} centralized metabolism, likely to avoid Fenton chemistry, which converts H_2O_2 to a more deleterious oxidant hydroxyl radical (7, 37). Although manganese, a first row transition metal, catalyzes Fenton-like reaction at acidic pH as well (38, 39), at physiological pH values it exhibits inorganic superoxide dismutase and catalase activities by complex with low molecular weight molecules, such as orthophosphate and bicarbonate (9, 10, 40). Manganese has been reported to help streptococci cope with oxidative stresses (4). Thus, intensive studies have been focused on how the streptococcal and other Firmicutes metalloregulator switch functions by sensing and binding the ligand metals (41, 42), e.g. the *S. pyogenes* MtsR and *S. mutans* SloR sense and regulate both cellular manganese and iron levels (29, 43), whereas the *S. gordonii* ScaR and *S. pneumoniae* PsaR function as the Mn^{2+}-sensitive regulators (24, 27, 28). Similar to ScaR and PsaR, the *S. oligofermentans* MntR also senses intracellular Mn^{2+} and then inhibits the expression of Mn^{2+} transporter operon *mntABC* (supplemental Table S2). Notably, this work demonstrates that So-MntR can be inactivated by H_2O_2 via oxidation of its redox sensitive cysteines (Figs. 2 and 3). H_2O_2 induces MntR to form Cys-11/Cys-11 and Cys-11/Cys-156 disulfide-linked dimers and oligomers, leading to a de-repression of *mntABC* expression and Mn^{2+} uptake for coping with the oxidative stress. This is supported by the fact that the *mntR*$_{So}$ mutant was more resistant to H_2O_2 injury than the wild type strain (Table 1). Deletion of *mntR*$_{So}$ also led to elevated intracellular iron (supplemental Table S1) but not decreased the H_2O_2 sensitivity of the bacterium. This can be attributed to the role of Dpr, a Fe^{2+} chelating protein, as an unpublished microarray analysis showed ~3-fold up-regulation of *dpr* in the *mntR*$_{So}$ inactivation mutant.[3]

To insight into the disulfide bond formation on protein conformation distortion, we, using SWISS-MODEL protein structure homology modeling server, performed a homology model of So-MntR protein and overlaid it with the dimeric crystal structure of the *S. gordonii* ScaR (3hrs.1.pdb, X-ray diffraction at 2.70 Å, Fig. 1*B*). The two proteins show an overall structural similarity. Based on this modeling structure of So-MntR, a distance of 25.67 Å was predicted between Cys-11 and Cys-156 within each monomer, whereas between monomers, distances of 55.69 Å and 41.83 Å for Cys-11/Cys-156, and Cys-11/Cys-11 were measured with PyMOL, respectively. Apparently, the predicted cysteine distances are much larger than 2.8 Å to allow for a disulfide-bond formation. Therefore, the identified Cys-11/Cys-11 or Cys-11/Cys-156 peptides in H_2O_2-treated So-MntR (Fig. 3*C*) strongly indicate a structure distortion of the H_2O_2-oxidized protein. According to the protein domain analysis (Fig. 1*A*) and structural study on *S. gordonii* ScaR (27), Cys-11 situates on the α1 helix associated to the DNA binding domain. This work shows that the Cys-11 thiol group exhibits high H_2O_2 reactivity to form intermolecular disulfide linkage with Cys-156 or Cys-11. Thus oxidation must change the protein into inactive form, which is supported by the *in vitro* EMSA data (Fig. 2, *B* and *C*).

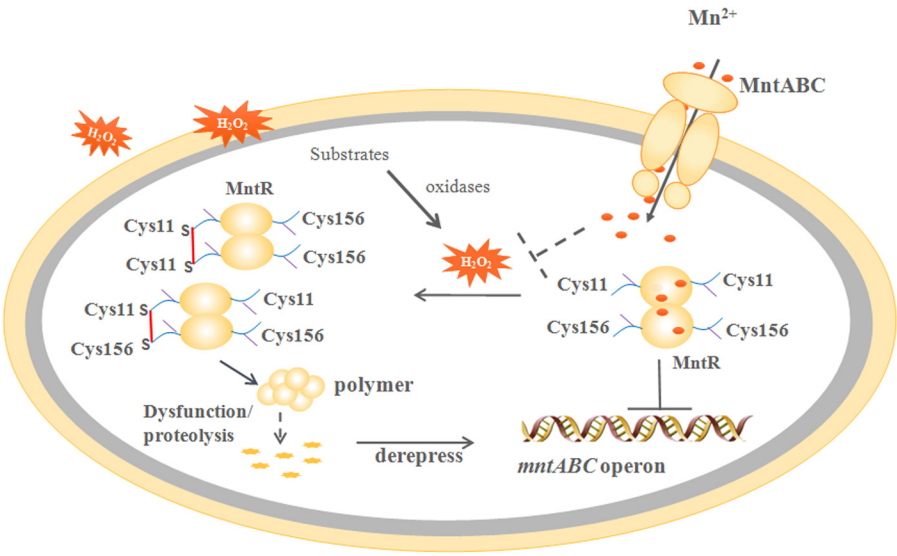

FIGURE 7. **A schematic working model of the streptococcal MntR in response to both Mn^{2+} and H_2O_2.** The metalloregulator MntR suppresses expression of the *mntABC* operon, which encodes the major Mn^{2+} ABC transporter MntABC, and so restricts manganese uptake by sensing the cellular manganese sufficiency. When encountering oxidative stress, MntR sacrifices itself, via the redox-reactive thiol group-mediated oligomerization and degradation, and releases *mntABC* expression to initiate the uptake of Mn^{2+} to cope with the oxidants. *Solid lines* specify the proved reactions, and *broken lines* represent predicted ones. *Yellow oval*, MntR protein; *red dot*, manganese ion; *purple* and *blue lines*, cysteine residue; *red lines*, disulfide bond.

Consistently, redox Western blot also detected oligomerization and degradation of the cellular So-MntR upon air exposure and H_2O_2 pulse (Fig. 5). This indicates that a bacterial surveillance system can sense the aberrant protein and initiate proteolysis to eliminate the dysfunctional So-MntR dimers and oligomers. Similar finding is reported for H_2O_2-mediated degradation of the uracil-DNA glycosylase (UNG1) in human mitochondria (44). Oxidized MntR degradation can also be similar to that oxidative carbonylation causes protein aggregation and degradation (45).

Therefore, a conclusion can be drawn that the metalloregulator MntR plays a dual role in controlling cellular manganese homeostasis. In the absence of oxidative stress, MntR, by sensing the cellular Mn^{2+} level, modulates Mn^{2+} uptake to meet the bacterium physiological requirement. When encountering oxidative stress, it "sacrifices" itself through redox-sensitive thiol group-mediated oligomerization to release suppression of *mntABC* for uptake Mn^{2+} to cope with the oxidants. The H_2O_2-reactive cysteine residue Cys-11, identified in *S. oligofermentans* MntR, is widely distributed in the DtxR family metalloregulators from streptococci (Fig. 1*A*). Although Cys-156 presents only in the MntR of *S. oligofermentans* and *S. lutetiensis*, a group of streptococcal DtxR homologues, including those derived from pathogen *S. pneumoniae*, *S. equi*, and *Streptococcus uberis*, contain a third cysteine at position 57 that associated to DNA binding domain. A preliminary study implemented in our laboratory found that upon H_2O_2 oxidation, the recombinant purified PsaR (spr1480) from *S. pneumoniae* formed disulfide-linked dimers as well. Further study is needed to extensively investigate the possible role of cysteines of these metalloregulators in H_2O_2 sensing in pathogenic streptococci. This mechanism would benefit the oral commensals and pathogenic streptococci, enabling them adapted to the oxidative tension in human ecological niches and, therefore, pathogenic.

Redox switches based on the redox-sensitive cysteine thiol groups have been widely utilized by H_2O_2 sensors in conducting the regulatory functions in response to reactive oxygen species that derived from the extracellular environments or respiratory metabolism. Those include the *E. coli* OxyR (46), the *Bacillus subtilis* OhrR (47) and the *Staphylococcus aureus* MgrA (48). In addition to the specialized redox regulators, recently quorum-sensing regulators, such as the *Pseudomonas aeruginosa* LasR (49), the *S. aureus* AgrA (50), and the *E. coli* SdiA (51) have been found to respond to oxidants via cysteine oxidation as well. Based on these findings and on that of the metalloregulator in this study, it is conceivable that any protein, including regulatory proteins, carrying redox-reactive thiol groups in cysteine or methionine residues can be involved in the regulation of redox reactions. Further studies on redox-sensitive cysteines at proteomics level are being implemented in our laboratory. These works would, therefore, much improve our understandings on how bacteria cope with oxidative stress via oxidizing protein post-translation modification.

Experimental Procedures

Bacterial Strains and Culture Condition—S. oligofermentans AS 1.3089 (52) and its derivative strains were grown in BHI broth (BD Difco, Franklin Lakes, NJ) statically or anaerobically under 100% N_2 at 37 °C. To test the effect of Mn^{2+} or Fe^{2+} on gene expression, $MnCl_2$ or $FeSO_4$ was supplemented to 5% Chelex 100 (C7901, Sigma)-treated BHI plus 0.1 mM $CaCl_2$ and 2 mM $MgCl_2$ (B-BHI). BHI plates supplemented with spectinomycin (1 mg ml^{-1}) or kanamycin (1 mg ml^{-1}) were used to select transformants. *E. coli* strains used for cloning and plasmid construction were grown in Luria-Bertani medium. Spectinomycin (250 μg ml^{-1}) or kanamycin (50 μg ml^{-1}) was used when necessary.

Construction of Genetic Strains—Genomic DNA of *S. oligofermentans* was extracted as described previously (53, 54). All primers (supplemental Table S4) were designed according to the genome sequence (33) and synthesized by Sangon Co. (Shanghai, China). $mntR_{So}$ deletion strain was constructed by the PCR ligation method (55). The upstream and downstream DNA fragments of $mntR_{So}$ were amplified using primer pairs listed in supplemental Table S4. The BamHI-digested PCR products were ligated with non-polar kanamycin resistance gene cassette released from plasmid pALH124 (56) and transformed into *S. oligofermentans* as described previously (54). Various $mntR_{So}$ gene ectopically expressed strains were constructed using the shuttle plasmid pDL278. A DNA fragment containing the promoter and six histidines tag-fused $mntR_{So}$ gene was PCR-amplified using the primer pair mntRcomF/mntRHiscomR, and the PCR product was inserted into the BamHI and HindIII sites of pDL278 to produce pDL278-*mntR*-His_6. Meanwhile, pDL278-*mntR*C11S-His_6, C123S-His_6, or C156S-His_6 was constructed using site-directed gene mutagenesis kit (Beyotime Biotechnology Co., Shanghai, China) and the mutagenesis primer pairs listed in supplemental Table S4. The correct recombinants were transformed into *S. oligofermentans* $mntR_{So}$ mutant. The P*mntABC* luciferase reporter in the $mntR_{So}$ mutant was constructed by deleting $mntR_{So}$ in the wild type P*mntABC-luc* fusion strain previously constructed (13). All the correct *S. oligofermentans* transformants were selected on BHI plates containing kanamycin or spectinomycin and identified by PCR and sequencing.

Overexpression and Purification of So-MntR Protein—A C-terminal fusion of His_6 to the So-MntR was constructed as follows. A 648-bp region containing the entire $mntR_{So}$ gene was PCR-amplified with primer pair mntR28aFNcoI/mntR28aRXhoI (supplemental Table S4). The resultant product was digested with NcoI/XhoI and ligated into the compatible sites on pET-28a (Novagen, Madison, WI) to produce pET-28a-mntR. The construct was verified by DNA sequencing. So-MntR C11S, C123S, and C156S mutants were constructed using the site mutagenesis kit and primers described above by using pET-28a-mntR as the template. The substitution of serine for cysteine was verified by sequencing. pET-28a carrying wild type or cysteine-mutated $mntR_{So}$ was transformed into *E. coli* BL21 (DE3) (Novagen) cells. Correct transformants were cultured in LB medium supplemented with 50 μg/ml kanamycin. Cells were grown at 37 °C to A_{600} of 0.4–0.6, and 0.5 mM isopropyl-β-D-thiogalactopyranoside (Sigma) was added. After an additional 3–4 h incubation, cells were collected by centrifugation at 8000 rpm for 10 min, resuspended in a 1/10 volume of binding buffer (20 mM sodium phosphate, 500 mM NaCl, 30 mM imidazole, 1 mM EDTA, 1 mM DTT, pH 7.4), and then lysed by sonication for 30 min. The cell lysate was centrifuged at 12,000 rpm for 15 min, and the supernatant was filtered through a 0.45-nm polyvinylidene difluoride membrane (Millipore, Billerica, MA) and then applied to a Ni^{2+}-charged chelating column (GE Healthcare) previously equilibrated with binding buffer. Proteins were eluted by elution buffer (20 mM sodium phosphate, 500 mM NaCl, 500 mM imidazole, 1 mM DTT, pH 7.4), and the elution fractions were analyzed by electrophoresis on a 12% sodium dodecyl sulfate-polyacrylamide gel. The fractions with desired protein were pooled and dialyzed against phosphate-buffered saline (PBS: 10 mM Na_2HPO_4, 1.8 mM KH_2PO_4, 137 mM NaCl, and 2.7 mM KCl, pH 7.4) containing 1 mM DTT and 1 mM EDTA 3 times, with the last dialysis in PBS containing 1 mM DTT and 10 g/liter Chelex 100. The purified proteins were stored in aliquots in 10% glycerol at −80 °C until use.

EMSA—The *mntABC* promoter fragment was generated by PCR amplification using a biotin-labeled primer pair of PmntEMSAF/PmntEMSAR (supplemental Table S4). EMSA was performed using Light Shift Chemiluminescent EMSA Kit (Pierce). Briefly, 0.2 nM biotin-labeled dsDNA probe and increasing amounts of So-MntRs (1–50 nM) were mixed in the binding buffer (10 mM Tris-HCl, pH 8.0, 5% glycerol, 50 mM NaCl, 10 μg/ml BSA, 2 ng/μl poly(dI-dC), 0.5 mM DTT, and 0.1 mM $MnCl_2$). The reaction remained at 30 °C for 30 min and then was electrophoresed on 8% polyacrylamide gel on ice. The DNA-protein complex was transferred onto a nylon membrane and detected by Chemiluminescent Nucleic Acid Detection Module kit (Thermo Scientific™).

Non-reducing SDS-PAGE—Five micrograms of So-MntR and its cysteine-mutated proteins were incubated with 0.1 or 1 mM H_2O_2 for 90 min at room temperature, respectively. Before electrophoresis, NEM (final concentration 40 mM) was added and put in the dark for 30 min. 4-Fold diluted non-reducing SDS loading buffer (0.2 M Tris-HCl, pH 6.8, 40% glycerol, 8% SDS, 0.4% bromphenol blue) was added, and then proteins were separated on 12% SDS-PAGE gel.

Redox Western Blot—Cells were collected by centrifugation and resuspended in RIPA buffer (50 mM Tris-HCl, pH 7.4, 150 mM NaCl, 1% Triton X-100, 1% sodium deoxycholate, 0.1% SDS, sodium orthovanadate, sodium fluoride, EDTA, leupeptin) with the addition of 40 mM NEM. After a 45-min sonication on ice using UP400S Ultrasonicator (Xinzi Co., Ningbo, China), the supernatant was collected by centrifugation. Protein concentration of the lysate was determined using the BCA protein measuring kit. Protein samples were diluted in non-reducing loading buffer (4×) (0.2 M Tris-HCl, pH 6.8, 40% glycerol, 8% SDS, 0.4% bromphenol blue). After heat denaturation, the proteins were separated by SDS-PAGE, transferred onto a nitrocellulose membrane, and hybridized with anti-His-tag antibody (Abmart Co., Shanghai, China) at a 4000-fold dilution. Detection was performed using the Chemiluminescent Nucleic Acid Detection Module kit.

LC-MS/MS Identification of Disulfide-linked Peptide—Non-reducing SDS-PAGE was used to separate H_2O_2-untreated and -treated So-MntR protein (total amount 5 μg/lane). After staining with Coomassie Blue G-250, the gel bands were cut into pieces. Gel pieces were washed twice with MS-grade water and directly alkylated with 55 mM iodoacetamide in the dark for 1 h at 37 °C and then digested by sequencing grade modified trypsin (Promega, Fitchburg, WI) in 50 mM NH_4HCO_3, pH 8.0, at 37 °C overnight. The digested products were extracted twice with 1% formic acid in 50% acetonitrile aqueous solution and dried to reduce volume by SpeedVac. For LC-MS/MS analysis, the peptides were separated by a 65-min gradient elution at a flow rate of 0.250 ml/min with the EASY-nLC integrated nano-HPLC system (Thermo-Fisher), which was directly interfaced

with the Thermo Q-Extractive mass spectrometer. The analytical column was a homemade fused silica capillary column (75-mm internal diameter, 150-mm length; Upchurch) packed with C-18 resin (300 Å, 5 μm; Varian). Mobile phase A consisted of 0.1% formic acid, and mobile phase B consisted of 100% acetonitrile and 0.1% formic acid. The Q-Extractive mass spectrometer was operated in the data-dependent acquisition mode using the Xcalibur 3.0 software. A single full-scan mass spectrum in the Orbitrap (300–1800 m/z, 70,000 resolution) was followed by 20 data-dependent MS/MS scans in the ion trap at 27% normalized collision energy. Each mass spectrum was searched against So-MntR protein sequence (Uniprot accession number N0C1Z2) using the SEQUEST searching engine of Proteome Discoverer software (v1.4). Peptide fragments with disulfide linkage were analyzed by PMi-Byonic software (Protein Matrix Inc.).

Cellular Metal Content Measurement—Concentrations of metal ions in static cultures of various *S. oligofermentans* strains were measured using ICP-MS. Overnight BHI cultures of tested strains were diluted 1:50 into fresh BHI broth and incubated at 37 °C under static conditions. Mid-log phase cells were harvested by centrifugation at 13,400 × g for 10 min. The cell pellets were washed twice in PBS with 1 mM EDTA and once in PBS without EDTA and then resuspended in 1 ml of PBS. 100 μl of suspension was used to measure protein concentration with a BCA protein analysis kit per the manufacturer's recommendations. The remaining 900 μl of suspension was collected by centrifugation at 13,400 × g for 10 min. Pelleted bacteria were resuspended in 500 μl of nitric acid (ultra pure). After incubation at room temperature overnight, the volume was brought to 1.5 ml with deionized distilled water. The samples were then analyzed for metal ions content with ICP-MS (DRCII, Perkin-Elmer Life Sciences) at Peking University Health Science Center. Beryllium, indium, and uranium were used as metal ions standard to calibrate ICP-MS. Experiments were conducted in triplicate, and each was repeated at least three times. Metal content was expressed in nmol/mg of protein.

Assay of Hydrogen Peroxide Sensitivity—Overnight cultures were 1:100 diluted into fresh BHI broth and incubated anaerobically. Until the growth reached $A_{600} \sim 0.5$–0.6, 0.2 ml of cells were harvested by centrifugation and then resuspended in 0.2 ml of fresh BHI broth. One aliquot (200 μl) was pulsed with 10 mM H_2O_2, leaving another aliquot not treated. After incubation at 37 °C for 10 min, cells from both samples were collected and washed twice with PBS buffer and resuspended in 200 μl of BHI broth. Cell chains were separated by sonication for 30 s with a XC-3200D ultrasonic cleaner (Xinchen Co., Nanjing, China) and then 10-fold series dilutions were performed. Appropriate dilutions were plated on BHI agar, and cfus were counted after 24 h incubation in a candle jar at 37 °C. The survival percentage was calculated by the cfus of the H_2O_2-challenged sample over those in controls. Experiments were executed in triplicate, and each was repeated at least three times independently.

Luciferase Activity Assay—Twenty-five microliters of 1 mM D-luciferin (Sigma) solution (in 1 mM citrate buffer, pH 6.0) was added to 100-μl sample, and luciferase assays were performed using a TD 20/20 luminometer (Turner Biosystems, Sunnyvale, CA). The optical density of the samples (A_{600}) was measured with a 2100 visible spectrophotometer (Unico, Shanghai, China) and used to normalize the luciferase activity. All the measurements were done for triplicate samples and repeated at least three times.

Quantitative PCR—Total RNA was extracted from mid-log phase ($A_{600} \sim 0.4$–0.5) cells using TRIzol reagent (Invitrogen) as recommended by the suppliers. After quality confirmation with a 1% agarose gel, the RNA was treated with RNase-free DNase (Promega, Madison, WI) and analyzed by PCR for possible chromosomal DNA contamination. cDNA was generated from 2 μg of total RNA with random primers using Moloney murine leukemia virus reverse transcriptase (Promega) according to the supplier's instructions and used for qPCR amplification with the corresponding primers (supplemental Table S4). Amplifications were performed with a Mastercycler ep realplex^2 (Eppendorf, Germany). To estimate copy numbers for a given mRNA, a standard curve of the tested gene was generated by quantitative PCR using 10-fold serially diluted PCR product as the template. The 16S rRNA gene was used as the biomass reference. The copy number of *mntA* gene was normalized to the number of 16S rRNA copies. The number of copies of the transcript of each gene per 1000 16S rRNA copies is shown.

Author Contributions—Z. C. expressed MntR, constructed the mutants, assayed redox status of MntR protein, and performed the H_2O_2 survivals of the strains. X. W., F. Y., and Q. H. prepared and characterized the MntR disulfide-linked peptides. H. T. and X. D. supervised the project and wrote the paper with input and approval from all authors.

Acknowledgments—We thank Drs. Zhenfeng Zhang and Jie Li at the Institute of Microbiology, CAS for helpful discussions on the work.

References

1. Aguirre, J. D., and Culotta, V. C. (2012) Battles with iron: manganese in oxidative stress protection. *J. Biol. Chem.* **287,** 13541–13548
2. Faulkner, M. J., and Helmann, J. D. (2011) Peroxide stress elicits adaptive changes in bacterial metal ion homeostasis. *Antioxid. Redox Signal.* **15,** 175–189
3. Martin, J. E., Waters, L. S., Storz, G., and Imlay, J. A. (2015) The *Escherichia coli* small protein MntS and exporter MntP optimize the intracellular concentration of manganese. *PLoS Genet.* **11,** e1004977
4. Turner, A. G., Ong, C. L., Gillen, C. M., Davies, M. R., West, N. P., McEwan, A. G., and Walker, M. J. (2015) Manganese homeostasis in group A *Streptococcus* is critical for resistance to oxidative stress and virulence. *mBio.* **6,** e00278–00315
5. Juttukonda, L. J., and Skaar, E. P. (2015) Manganese homeostasis and utilization in pathogenic bacteria. *Mol. Microbiol.* **97,** 216–228
6. Eijkelkamp, B. A., McDevitt, C. A., and Kitten, T. (2015) Manganese uptake and streptococcal virulence. *Biometals* **28,** 491–508
7. Ogunniyi, A. D., Mahdi, L. K., Jennings, M. P., McEwan, A. G., McDevitt, C. A., Van der Hoek, M. B., Bagley, C. J., Hoffmann, P., Gould, K. A., and Paton, J. C. (2010) Central role of manganese in regulation of stress responses, physiology, and metabolism in *Streptococcus pneumoniae. J. Bacteriol.* **192,** 4489–4497
8. Archibald, F. S., and Fridovich, I. (1981) Manganese, superoxide-dismutase, and oxygen tolerance in some lactic-acid bacteria. *J. Bacteriol.* **146,** 928–936

9. Stadtman, E. R., Berlett, B. S., and Chock, P. B. (1990) Manganese-dependent disproportionation of hydrogen peroxide in bicarbonate buffer. *Proc. Natl. Acad. Sci. U.S.A.* **87,** 384–388
10. Barnese, K., Gralla, E. B., Cabelli, D. E., and Valentine, J. S. (2008) Manganous phosphate acts as a superoxide dismutase. *J. Am. Chem. Soc.* **130,** 4604–4606
11. Daly, M. J. (2009) A new perspective on radiation resistance based on *Deinococcus radiodurans*. *Nat. Rev. Microbiol.* **7,** 237–245
12. Jakubovics, N. S., Smith, A. W., and Jenkinson, H. F. (2002) Oxidative stress tolerance is manganese (Mn^{2+}) regulated in *Streptococcus gordonii*. *Microbiology* **148,** 3255–3263
13. Wang, X., Tong, H., and Dong, X. (2014) PerR-regulated manganese ion uptake contributes to oxidative stress defense in an oral streptococcus. *Appl. Environ. Microbiol.* **80,** 2351–2359
14. Helmann, J. D. (2014) Specificity of metal sensing: iron and manganese homeostasis in *Bacillus subtilis*. *J. Biol. Chem.* **289,** 28112–28120
15. Jakubovics, N. S., and Jenkinson, H. F. (2001) Out of the iron age: new insights into the critical role of manganese homeostasis in bacteria. *Microbiology* **147,** 1709–1718
16. Merchant, A. T., and Spatafora, G. A. (2014) A role for the DtxR family of metalloregulators in gram-positive pathogenesis. *Mol. Oral. Microbiol.* **29,** 1–10
17. Que, Q., and Helmann, J. D. (2000) Manganese homeostasis in *Bacillus subtilis* is regulated by MntR, a bifunctional regulator related to the diphtheria toxin repressor family of proteins. *Mol. Microbiol.* **35,** 1454–1468
18. Rolerson, E., Swick, A., Newlon, L., Palmer, C., Pan, Y., Keeshan, B., and Spatafora, G. (2006) The SloR/Dlg metalloregulator modulates *Streptococcus mutans* virulence gene expression. *J. Bacteriol.* **188,** 5033–5044
19. Reyes-Caballero, H., Campanello, G. C., and Giedroc, D. P. (2011) Metalloregulatory proteins: metal selectivity and allosteric switching. *Biophys. Chem.* **156,** 103–114
20. Huang, X., Shin, J. H., Pinochet-Barros, A., Su, T. T., and Helmann, J. D. (2017) *Bacillus subtilis* MntR coordinates the transcriptional regulation of manganese uptake and efflux systems. *Mol. Microbiol.* **103,** 253–268
21. O'Rourke, K. P., Shaw, J. D., Pesesky, M. W., Cook, B. T., Roberts, S. M., Bond, J. P., and Spatafora, G. A. (2010) Genome-wide characterization of the SloR metalloregulome in *Streptococcus mutans*. *J. Bacteriol.* **192,** 1433–1443
22. Olsen, R. J., Sitkiewicz, I., Ayeras, A. A., Gonulal, V. E., Cantu, C., Beres, S. B., Green, N. M., Lei, B., Humbird, T., Greaver, J., Chang, E., Ragasa, W. P., Montgomery, C. A., Cartwright, J., Jr, McGeer, A., *et al.* (2010) Decreased necrotizing fasciitis capacity caused by a single nucleotide mutation that alters a multiple gene virulence axis. *Proc. Natl. Acad. Sci. U.S.A.* **107,** 888–893
23. Haswell, J. R., Pruitt, B. W., Cornacchione, L. P., Coe, C. L., Smith, E. G., and Spatafora, G. A. (2013) Characterization of the functional domains of the SloR metalloregulatory protein in *Streptococcus mutans*. *J. Bacteriol.* **195,** 126–134
24. Jakubovics, N. S., Smith, A. W., and Jenkinson, H. F. (2000) Expression of the virulence-related Sca (Mn^{2+}) permease in *Streptococcus gordonii* is regulated by a diphtheria toxin metallorepressor-like protein ScaR. *Mol. Microbiol.* **38,** 140–153
25. Johnston, J. W., Briles, D. E., Myers, L. E., and Hollingshead, S. K. (2006) Mn^{2+}-dependent regulation of multiple genes in *Streptococcus pneumoniae* through PsaR and the resultant impact on virulence. *Infect. Immun.* **74,** 1171–1180
26. Kloosterman, T. G., Witwicki, R. M., van der Kooi-Pol, M. M., Bijlsma, J. J., and Kuipers, O. P. (2008) Opposite effects of Mn^{2+} and Zn^{2+} on PsaR-Mediated expression of the virulence genes *pcpA*, *prtA*, and *psaBCA* of *Streptococcus pneumoniae*. *J. Bacteriol.* **190,** 5382–5393
27. Stoll, K. E., Draper, W. E., Kliegman, J. I., Golynskiy, M. V., Brew-Appiah, R. A., Phillips, R. K., Brown, H. K., Breyer, W. A., Jakubovics, N. S., Jenkinson, H. F., Brennan, R. G., Cohen, S. M., and Glasfeld, A. (2009) Characterization and structure of the manganese-responsive transcriptional regulator ScaR. *Biochemistry* **48,** 10308–10320
28. Lisher, J. P., Higgins, K. A., Maroney, M. J., and Giedroc, D. P. (2013) Physical characterization of the manganese-sensing pneumococcal surface antigen repressor from *Streptococcus pneumoniae*. *Biochemistry* **52,** 7689–7701
29. Spatafora, G., Corbett, J., Cornacchione, L., Daly, W., Galan, D., Wysota, M., Tivnan, P., Collins, J., Nye, D., Levitz, T., Breyer, W. A., and Glasfeld, A. (2015) Interactions of the metalloregulatory protein SloR from *Streptococcus mutans* with its metal ion effectors and DNA binding site. *J. Bacteriol.* **197,** 3601–3615
30. Tong, H., Chen, W., Merritt, J., Qi, F., Shi, W., and Dong, X. (2007) *Streptococcus oligofermentans* inhibits *Streptococcus mutans* through conversion of lactic acid into inhibitory H_2O_2: a possible counteroffensive strategy for interspecies competition. *Mol. Microbiol.* **63,** 872–880
31. Tong, H., Chen, W., Shi, W., Qi, F., and Dong, X. (2008) SO-LAAO, a novel L-amino acid oxidase that enables *Streptococcus oligofermentans* to outcompete *Streptococcus mutans* by generating H_2O_2 from peptone. *J. Bacteriol.* **190,** 4716–4721
32. Liu, L., Tong, H., and Dong, X. (2012) Function of the pyruvate oxidase-lactate oxidase cascade in interspecies competition between *Streptococcus oligofermentans* and *Streptococcus mutans*. *Appl. Environ. Microbiol.* **78,** 2120–2127
33. Tong, H., Shang, N., Liu, L., Wang, X., Cai, J., and Dong, X. (2013) Complete genome sequence of an oral commensal, *Streptococcus oligofermentans* strain AS 1.3089. *Genome Announc.* **1,** e00353-e00413
34. LeBlanc, D. J., Lee, L. N., and Abu-Al-Jaibat, A. (1992) Molecular, genetic, and functional analysis of the basic replicon of pVA380–1, a plasmid of oral streptococcal origin. *Plasmid* **28,** 130–145
35. Jin, D., Chen, C., Li, L., Lu, S., Li, Z., Zhou, Z., Jing, H., Xu, Y., Du, P., Wang, H., Xiong, Y., Zheng, H., Bai, X., Sun, H., Wang, L., *et al.* (2013) Dynamics of fecal microbial communities in children with diarrhea of unknown etiology and genomic analysis of associated *Streptococcus lutetiensis*. *BMC Microbiol.* **13,** 141
36. Boyd, J., Oza, M. N., and Murphy, J. R. (1990) Molecular cloning and DNA sequence analysis of a diphtheria tox iron-dependent regulatory element (*dtxR*) from *Corynebacterium diphtheriae*. *Proc. Natl. Acad. Sci. U.S.A.* **87,** 5968–5972
37. Pericone, C. D., Park, S., Imlay, J. A., and Weiser, J. N. (2003) Factors contributing to hydrogen peroxide resistance in *Streptococcus pneumoniae* include pyruvate oxidase (SpxB) and avoidance of the toxic effects of the fenton reaction. *J. Bacteriol.* **185,** 6815–6825
38. Watts, R. J., Sarasa, J., Loge, F. J., and Teel, A. L. (2005) Oxidative and reductive pathways in manganese-catalyzed Fenton's reactions. *J. Environ. Eng.* **131,** 158–164
39. Goldstein, S., and Meyerstein, D. (1999) Comments on the mechanism of the "Fenton like" reaction. *Acc. Chem. Res.* **32,** 547–550
40. Archibald, F. S., and Fridovich, I. (1982) The scavenging of superoxide radical by manganous complexes: *in vitro*. *Arch. Biochem. Biophys.* **214,** 452–463
41. Guerra, A. J., and Giedroc, D. P. (2012) Metal site occupancy and allosteric switching in bacterial metal sensor proteins. *Arch. Biochem. Biophys.* **519,** 210–222
42. McGuire, A. M., Cuthbert, B. J., Ma, Z., Grauer-Gray, K. D., Brunjes Brophy, M., Spear, K. A., Soonsanga, S., Kliegman, J. I., Griner, S. L., Helmann, J. D., and Glasfeld, A. (2013) Roles of the A and C sites in the manganese-specific activation of MntR. *Biochemistry* **52,** 701–713
43. Bates, C. S., Toukoki, C., Neely, M. N., and Eichenbaum, Z. (2005) Characterization of MtsR, a new metal regulator in group A streptococcus, involved in iron acquisition and virulence. *Infect. Immun.* **73,** 5743–5753
44. Liu, Z., Hu, Y., Gong, Y., Zhang, W., Liu, C., Wang, Q., and Deng, H. (2016) Hydrogen peroxide mediated mitochondrial UNG1-PRDX3 interaction and UNG1 degradation. *Free. Radic. Biol. Med* **99,** 54–62
45. Dahl, J. U., Gray, M. J., and Jakob, U. (2015) Protein quality control under oxidative stress conditions. *J. Mol. Biol* **427,** 1549–1563
46. Zheng, M., Aslund, F., and Storz, G. (1998) Activation of the OxyR transcription factor by reversible disulfide bond formation. *Science* **279,** 1718–1721
47. Fuangthong, M., and Helmann, J. D. (2002) The OhrR repressor senses organic hydroperoxides by reversible formation of a cysteine-sulfenic acid derivative. *Proc. Natl. Acad. Sci. U.S.A.* **99,** 6690–6695

48. Chen, P. R., Brugarolas, P., and He, C. (2011) Redox signaling in human pathogens. *Antioxid. Redox Signal.* **14,** 1107–1118
49. Kafle, P., Amoh, A. N., Reaves, J. M., Suneby, E. G., Tutunjian, K. A., Tyson, R. L., and Schneider, T. L. (2016) Molecular insights into the impact of oxidative stress on the quorum-sensing regulator protein LasR. *J. Biol. Chem.* **291,** 11776–11786
50. Sun, F., Liang, H., Kong, X., Xie, S., Cho, H., Deng, X., Ji, Q., Zhang, H., Alvarez, S., Hicks, L. M., Bae, T., Luo, C., Jiang, H., and He, C. (2012) Quorum-sensing agr mediates bacterial oxidation response via an intramolecular disulfide redox switch in the response regulator AgrA. *Proc. Natl. Acad. Sci. U.S.A.* **109,** 9095–9100
51. Kim, T., Duong, T., Wu, C. A., Choi, J., Lan, N., Kang, S. W., Lokanath, N. K., Shin, D., Hwang, H. Y., and Kim, K. K. (2014) Structural insights into the molecular mechanism of *Escherichia coli* SdiA, a quorum-sensing receptor. *Acta Crystallogr. D Biol. Crystallogr.* **70,** 694–707
52. Tong, H., Gao, X., and Dong, X. (2003) *Streptococcus oligofermentans* sp nov., a novel oral isolate from caries-free humans. *Int. J. Syst. Evol. Microbiol* **53,** 1101–1104
53. Dong, X., Xin, Y., Jian, W., Liu, X., and Ling, D. (2000) *Bifidobacterium thermacidophilum* sp nov., isolated from an anaerobic digester. *Int. J. Syst. Evol. Microbiol* **50,** 119–125
54. Tong, H., Zhu, B., Chen, W., Qi, F., Shi, W., and Dong, X. (2006) Establishing a genetic system for ecological studies of *Streptococcus oligofermentans*. *FEMS. Microbiol. Lett.* **264,** 213–219
55. Lau, P. C., Sung, C. K., Lee, J. H., Morrison, D. A., and Cvitkovitch, D. G. (2002) PCR ligation mutagenesis in transformable streptococci: application and efficiency. *J. Microbiol. Methods* **49,** 193–205
56. Liu, Y., Zeng, L., and Burne, R. A. (2009) AguR is required for induction of the *streptococcus mutans* agmatine deiminase system by low pH and agmatine. *Appl. Environ. Microbiol.* **75,** 2629–2637